

Nanosecond source of coherent radiation of the 2.65–5.29 μm spectral range for lidar systems

Tie-June Wang,¹ Zhenghui Kan,¹ Jin-Yue Gao,¹ Yu.M. Andreev,²
G.V. Lanskii,² and A.V. Shaiduko²

¹Key Laboratory of Coherent Light and Atomic and Molecular Spectroscopy of Ministry of Education and
College of Physics, Jilin University, Changchun, China

²Institute of Monitoring of Climatic and Ecological Systems,
Siberian Branch of the Russian Academy of Sciences, Tomsk, Russia

Received February 12, 2007

The available and experimentally obtained data on phase matching in AgGaS₂ crystals are analyzed. Model and experimental results for OPO and TWO of type I are presented. The radiation spectrum of nanosecond OPO overlaps the 2.65–5.29 μm range at a long-term operation stability and in the absence of saturation effect in the output power. Best-fit Sellmeier equations for AgGaS₂ are identified among the available ones.

Introduction

Frequency converters for visible – near IR and near IR – middle IR ranges, based on different nonlinear crystals, are widely used in lidar systems. At present, high-efficiency frequency converters of near IR lasers are of increasing interest for main atmospheric transparency windows of 3–5 and 7.5–9 μm , promising, in particular, for lidar gas-analyzers. Together with commercial frequency converters to the Visible and UV, they can serve as a base for ultra-wideband sources of 0.2–14 μm radiation appropriate to development of universal lidar systems. Unfortunately, effective nonlinear mid-IR crystals, particularly, CdGeAs₂, ZnGeP₂, Tl₃AsSe₃, and AgGaSe₂ are non-transparent and have large optical losses at wavelengths of near IR lasers,¹ which restricts the possibilities of development and the efficiency of their frequency conversion to the mid-IR range.

In contrast to these crystals, negative AgGaS₂ crystals with point symmetry group $\bar{4}2m$ are zero-level transparent within the 0.47–13 μm , i.e., throughout the near IR spectral range and the most part of the visible one. This minimizes both linear and nonlinear two-photon optical losses for lasers with $\lambda \geq 1 \mu\text{m}$. Therefore, many works are devoted to study optical parametric oscillators (OPO) and traveling wave oscillators (TWO) based on the AgGaS₂ crystals pumped by nano- and picosecond near-IR dye lasers, as well as different Nd:YAG and femtosecond Ti:sapphire and Cr:forsterite lasers.^{1–11} In particular, the generation spectrum of ps TWO of I type, based on two sequential crystals of 15 and 30 cm in length, overlaps wide 1.2–10 μm range⁴

with a quantum efficiency up to 10% and an idler wave pulse energy of $\leq 0.3 \text{ mJ}$ in the 3–5 μm range; the generation spectrum of ns single-resonant OPO of II type with nonselective resonator overlaps the 3.9–11.3 μm range.³ In the last case, crystal interaction of the type II is preferable due to larger (by 25–30%) effective nonlinear susceptibility as compared to that of I type. The generation spectrum of ns OPO of I type fails to overlap the whole 3–5 μm range, as well as to exceed the 0.1-mJ level of the input pulse energy.

The frequency-conversion efficiency seldom exceeds tenth fractions or units of percents^{3,5,6} because of two reasons. First, the second-order coefficient of nonlinear susceptibility $d_{36} = 12.5 \text{ pm/V}$, minimal among IR-transparent crystals, requires a highly intensive pumping. Second, minimal coefficients of thermal conductivity $\kappa = 0.0014$ and $0.0015 \text{ W/(cm}\cdot\text{K)}$, parallel and normal to the optical axis, cause the crystal destruction in attempting to overcome the reached limits of the generation range and output pulse energy parameters.⁵

Note also that despite the fact that at least six full sets of dispersion equations are known and used for calculations of phase-matching conditions,^{1–11} the problem of choice of a reliable system for calculations remains open.

Recent commercial AgGaS₂ crystals of high optical quality (summary coefficient of optical loss $\alpha \leq 0.001 \text{ cm}^{-1}$ at $\lambda = 1.06 \mu\text{m}$)² and techniques for producing high-quality antireflection coatings allow a detail analysis of phase matching conditions and estimation of new possibilities in the designing on their basis of OPO/TWO operating in the 3–5 μm range.

1. Analysis of phase matching conditions

The following Sellmeier equations for AgGaS₂ crystals are known:

$$\begin{aligned} n_o^2 &= 5.728 + \frac{0.2410}{\lambda^2 - 0.0870} - 0.00210\lambda^2, \\ n_e^2 &= 5.497 + \frac{0.2026}{\lambda^2 - 0.1307} - 0.00233\lambda^2, \end{aligned} \quad (1)$$

$$\lambda = 0.5\text{--}13 \mu\text{m} \text{ [Ref. 10]},$$

$$\begin{aligned} n_o^2 &= 2.6149 + \frac{3.1769\lambda^2}{\lambda^2 - 0.0739} + \frac{2.1328\lambda^2}{\lambda^2 - 950.0}, \\ n_e^2 &= 3.0398 + \frac{2.4973\lambda^2}{\lambda^2 - 0.0912} + \frac{2.1040\lambda^2}{\lambda^2 - 950.0}, \end{aligned} \quad (2)$$

$$\lambda = 0.5\text{--}13 \mu\text{m} \text{ [Ref. 9]},$$

$$n_o^2 = 3.3970 + \frac{2.3982}{1 - 0.09311/\lambda^2} + \frac{2.1640}{1 - 950.0/\lambda^2} \text{ [Ref. 5]}, \quad (3)$$

$$n_e^2 = 3.5873 + \frac{1.9533}{1 - 0.11066/\lambda^2} + \frac{2.3391}{1 - 1030.7/\lambda^2},$$

$$\begin{aligned} n_o^2 &= 5.814100 + \\ &+ \frac{0.0867547}{\lambda^{3.156983} - 0.0356502} + \frac{\lambda^{2.225043} 176380.0}{\lambda^{2.225043} - 112586195.0} + \\ &+ \frac{0.0821721}{\lambda^{4.430430} + 0.315646} + \frac{0.506566}{\lambda^{6.604280} + 6.582197}, \end{aligned} \quad (4)$$

$$\begin{aligned} n_e^2 &= 5.530050 + \frac{0.0510941}{\lambda^{2.359877} - 0.141109} + \\ &+ \frac{\lambda^{2.383834} 4253.78}{\lambda^{2.383834} - 4304924.0} + \frac{0.195314}{\lambda^{2.566664} + 0.0910735}, \\ \lambda &= 0.49\text{--}12 \mu\text{m} \text{ [Ref. 7]}, \end{aligned}$$

$$\begin{aligned} n_o^2 &= 5.79419 + \frac{0.23114}{\lambda^2 - 0.06882} - 2.4534 \cdot 10^{-3} \lambda^2 + \\ &+ 3.1814 \cdot 10^{-7} \lambda^4 - 9.7051 \cdot 10^{-9} \lambda^6, \\ n_e^2 &= 5.54120 + \frac{0.22041}{\lambda^2 - 0.09824} - 2.5240 \cdot 10^{-3} \lambda^2 + \\ &+ 3.6214 \cdot 10^{-7} \lambda^4 - 8.3605 \cdot 10^{-9} \lambda^6, \end{aligned} \quad (5)$$

$$0.54 \mu\text{m} < \lambda < 12.9 \mu\text{m} \text{ [Refs. 6, 8]},$$

where λ is the wavelength; n_o and n_e are the refractivity of ordinary and extraordinary waves, respectively.

Birefringence dispersions, calculated by Eqs. (1)–(5), are shown in Fig. 1.

Birefringence minima, assessed by equations from Ref. 10, and maxima, assessed by equations from Ref. 7, yield the phase-matching estimation curves giving the maximal and minimal angles of phase matching for OPO of type I almost throughout the phase-matching range (Fig. 2).

In particular, in the spectral regions, close to degeneracy points, the phase matching angles, calculated according to Ref. 10, are several degrees higher than all known experimental results; the results, estimated by data from Ref. 5 insignificantly exceed those from Ref. 7.

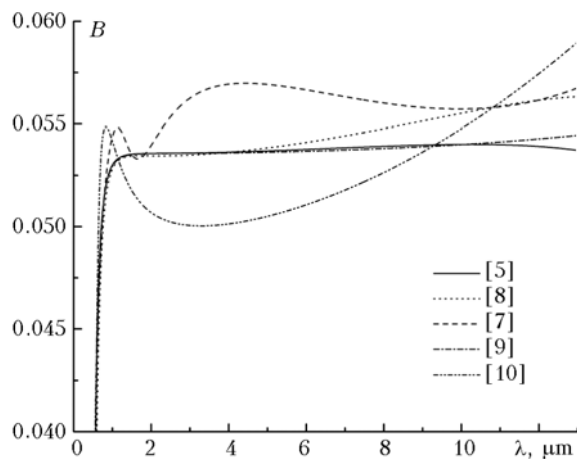


Fig. 1. Spectral dependence of birefringence factors.

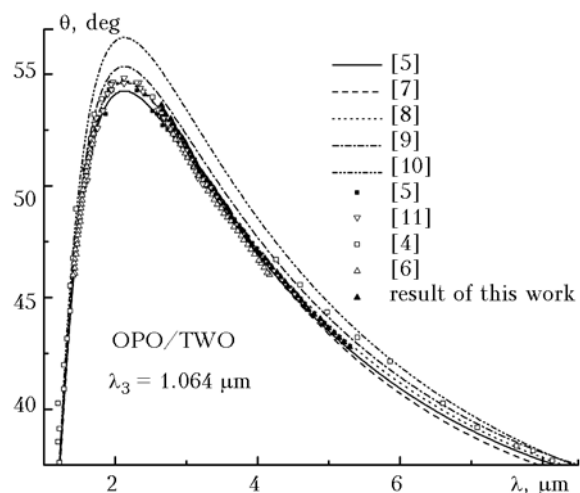


Fig. 2. Phase-matching curves for Nd:YAG-laser pumped OPO/TWO of type I. Markers correspond to experimental results.

In their turn, data from Refs. 7 and 8 noticeably differing in birefringence value at the most part of the analyzed range, give virtually equal values of phase-matching angles both at the degeneracy point and in the rest of the phase-matching range. The conclusion can be drawn from Fig. 2, that experimental angles of phase matching for OPO of type I are mostly agree with estimates by the dispersion data.⁸ For OPO of type II, phase-matching curves differ far less up to $\lambda < 10.5 \mu\text{m}$, and the spectral dependence of the experimental data completely follows the dependences, estimated by data from Refs. 7 and 8. However, in this case, the experimental data on phase-matching angles⁸ throughout the measurement range are closer by approximately 1° to the estimations from Ref. 7.

2. Experiment

In this work, a nanosecond OPO of type I, built according to an ordinary optical scheme, is studied. A nanosecond electrooptical Q-switch Nd:YAG laser of our own design was used as a pump laser. Its output parameters are the following: the diameter of output TEM₀₀ beam is 1.4 mm, the half-height pulse width (FWHM) is 8–10 ns, the pulse energy is up to 100 mJ, the pulse repetition rate is up to 10 Hz. The pumping pulse energy was controlled by a quarter-wave plate, Glan prism, attenuators, and varying supply voltage. Energy distribution in the pump beam cross section was controlled with a digital IR video camera. Crystal adjustment to the phase-matching direction with a precision of 4.5" was carried out with a computer-controlled RCA100 positioner (Zolix Instruments Co., Ltd, China), equipped with a step motor. The generated radiation wavelength was determined with a computer-controlled UV-DIL SBP300 monochromator (Zolix Instruments Co., Ltd, China) with a grating of 66 dash/mm. Radiation pulses were recorded with a nitrogen-cooled SRT photoconductor (area of sensitivity is 0.5 × 0.5 mm and time constant is about 10 ns) or a piezoelectric PCI-L-3 detector (Vigo System S.A., Poland) (spectral sensitivity range is 2–12 μm, area of sensitivity is 1 × 1 mm, time constant is less than 1 ns). Temporal behavior of the recorded pulses was analyzed with a digital two-channel TDS3052 oscillograph (Tektronix Inc.) having a pass band of 500 MHz and a time constant of 1.3 ns. The pulse energy was measured with a calibrated piezoelectric detector.

In this experiment, an antireflection AgGaS₂ crystal (MolTech GmbH, Germany) of 10 × 7 × 20 mm in size with the orientation $\theta = 47^\circ$ and $\varphi = 45^\circ$ was used for interactions of type I. The coefficient of crystal optical loss $\alpha < 0.005 \text{ cm}^{-1}$ at the Nd:YAG laser wavelengths within the region of maximal transparency was determined with a Fourier spectrometer Avatar 360 FTIR, Nicolet, USA (2.5–25 μm, a spectral resolution of 4 cm⁻¹). Working antireflection surface of the crystal had a high transparency (HT) at a pumping wavelength of 1.06 μm (HT_{1.06} > 98%), as well as at wavelengths of signal (HT_{1.3–1.7} > 99.5%) and idler (HT_{3–5} > 95%) branches of parametric generation. Both dielectric mirrors of OPO cavity are similar, with HT_{1.06} > 98%, HR_{1.3–1.7} > 99–99.4%, and HT_{3–5} > 88–98%.

When OPO ns-pulse pumping, the long-term stable generation of idler wavelengths within the 2.65–5.29 μm range with an output pulse energy up to 0.32 mJ, free of some saturation effect indications, was obtained. The dependence of OPO output pulse energy on the pump energy is exemplified in Fig. 3.

The pump energy increase by 15–20% due to the use of an optic amplifier with the coefficient of amplification $G \geq 3$ resulted in indications of output pulse energy saturation and destruction of dielectric mirrors after the OPO operation during several

hours. The 1.5-fold increase of pump beam diameter with preserving the peak pump intensity allowed almost doubling of the OPO output pulse energy. In case of using a dispersive prism with an acute angle of 30°, with the same antireflection quality as the nonlinear crystal, the generation range became almost halved. According to our data, the spectrum of ns OPO of I type, based on AgGaS₂ crystals, for the first time totally overlaps the range of main atmospheric transparency window of 3–5 μm, and the maximal energy of ns-pulses at the wavelengths of idler generation path is gained. As well, the OPO with selective cavity has been activated for the first time.

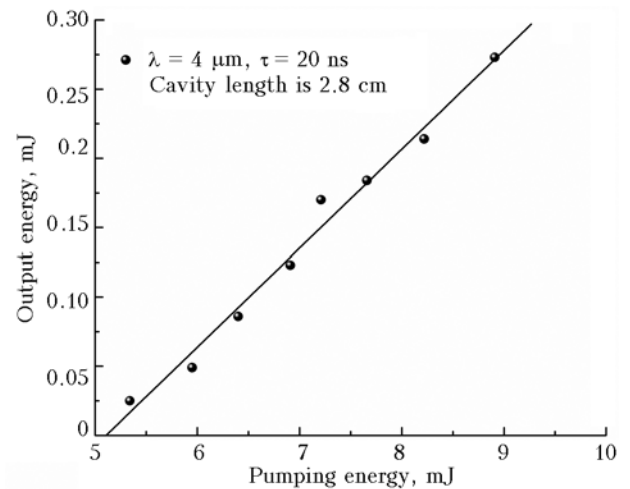


Fig. 3. Output pulse energy of the idler OPO wave as a function of the pump energy.

The experimental data on angles of phase matching (see Fig. 2) are in good agreement with estimates by the data from Ref. 8 and completely repeat the spectral behavior of experimental data⁶ for a crystal of the same producer. Absolute values of phase matching angles in this case exceed the values, given in Ref. 6, by 20', which is within the crystal cutting precision. When approaching degeneracy points, experimentally determined angles of phase matching have a tendency of displacing to the phase-matching curve, calculated by data from Ref. 9. The same conclusion can be also drawn for the experimental data from Ref. 4 and, probably, Refs. 5 and 11.

A rhodamine 6G passive mode locking Nd:YAG laser of our design, with amplifier ($G > 3$), generating a train of 8–13 isolated 100-ps pulses (FWHM) with 6.2-ns interval, (80 ± 20)-ns envelope length, and summarized train energy of 2–3 mJ, did not allow us to register TWO because of surface damages of the crystal and OPO mirrors. It was found that the AgGaS₂ crystal resistance to mode-locking pulses is only 5–6 times higher than to smooth pulses of the same duration.

The effect of parametric generation was registered in the 3.1 μm region when using as a pumping source the OPO with a ring cavity of

passive/active mode locking Nd:YAG laser, generating a train of 100–120 pulses not longer than 350 ps. Pumping of the second non-antireflection AgGaS₂ crystal of 5 × 5 × 3 mm in size (EKSMA Co., Lithuania) with 230-fs Ti:sapphire laser radiation of our own design easily allows us to obtain TWO. These parametric devices will be described in detail in a specially written paper.

Conclusion

According to available information, a nanosecond AgGaS₂ OPO of type I has been first activated; it completely overlaps the main atmospheric transparency window in a range from 3 to 5 μm. OPO performances allow the device to be used in lidar systems. At maximum pulse energy up to 0.56 mJ, it overlaps a range 2.65–5.29 μm. A nanosecond AgGaS₂ OPO with a selective cavity has been designed. The best-fit Sellmeier equations are identified, which are to be corrected to better agreement between the estimation results and experimentally determined angles of phase matching for OPO of the type I in the vicinity of the degeneracy point.

Reference

1. G.G. Gurzadyan, V.G. Dmitriev, and D.N. Nikogosyan, *Handbook on Nonlinear Optical Crystals* (Springer Series in Optical Sciences, Berlin, 1999), V. 64, 413 pp.
2. A. Douillet, J.J. Zondy, A. Yeliseev, S. Lobanov, and L. Isaenko, *J. Opt. Soc. Am. B* **16**, No. 9, 1481–1498 (1999).
3. K.L. Vodopyanov, J.P. Maffetone, I. Zwieback, and W. Ruderman, *Appl. Phys. Lett.* **75**, No. 9, 1204–1206 (1999).
4. T. Elsaesser, A. Seilmeier, W. Kaiser, P. Koidl, and G. Brandt, *Appl. Phys. Lett.* **44**, No. 4, 383–385 (1984).
5. Y.X. Fan, R.C. Eckard, R.L. Byer, R.K. Route, and R.S. Feigelson, *Appl. Phys. Lett.* **45**, No. 4, 313–315 (1984).
6. P.P. Boon, W.R. Fen, C.T. Chong, and X.B. Xi, *Jap. J. Appl. Phys.* **36**, No. 12B, 1661–1664 (1997).
7. D.A. Roberts, *Appl. Opt.* **35**, No. 24, 4677–4688 (1996).
8. A. Harasaki and K. Kato, *Jap. J. Appl. Phys.* **36**, No. 2, 700–703 (1997).
9. G. Bhar and R.C. Smith, *IEEE J. Quantum. Electron.* **10**, No. 7, 546–550 (1974).
10. D.S. Chemla, P.J. Kupecek, D.S. Robertson, and R.C. Smith, *Opt. Commun.* **3**, No. 1, 29–31 (1971).
11. G.C. Bhar, S. Das, D.K. Ghosh, and L.K. Samanta, *IEEE J. Quantum. Electron.* **24**, No. 8, 1492–1494 (1988).